



Supplement of

Dissolved organic matter fosters core mercury-methylating microbiomes for methylmercury production in paddy soils

Qiang Pu et al.

Correspondence to: Bo Meng (mengbo@mail.gyig.ac.cn)

The copyright of individual parts of the supplement might differ from the article licence.

1 **Supplementary Texts**

2 **S1. Measurement of soil physico-chemical properties, mercury and dissolved organic matter.**

3 **S1.1 Characterization of soil physico-chemical properties.**

4 Soil pH was measured using a pH meter (PD-501, SANXIN, China) after extracting 10 g of soil with
5 ultrapure deionized water (soil: water = 1:2.5 w/v). Soil total carbon and total nitrogen were measured by
6 an organic elemental analyzer (vario MACRO cube, Elementar, Germany) using 0.05 g of soil samples.
7 Water-soluble SO_4^{2-} was extracted from 1 g of soil with ultrapure deionized water in a 1:10 w/v ratio
8 using a horizontal oscillator at 220 rpm for 16 h in the dark. The supernatant solution was obtained by
9 centrifugation ($2500 \times g$ for 10 min) and filtration (0.45 μm , PES, Bizcomr, China). Water-soluble SO_4^{2-}
10 was analyzed with a UV-Vis spectrophotometer (UV-5100B, METASH, China). Water-soluble NO_3^- was
11 extracted from 1 g of soil with 50 mL of 2 M KCl, then filtered using PES membranes (0.45 μm , Bizcomr,
12 China), and measured by UV spectrophotometry (UV-1200, Macy Analysis Instrument Co. Ltd., China).
13 The S^{2-} and Fe^{2+} in soil pore water were obtained by centrifuging fresh soil samples in 50 mL centrifuge
14 tubes at $3500 \times g$ for 15 minutes. The S^{2-} in soil pore water was measured by using methylene blue
15 method (Cline, 1969), with a detection limit of 0.13 μM . The Fe^{2+} in soil pore water was measured by
16 using ferrozine method (Viollier et al., 2000), with a detection of 10 μM .

17 **S1.2 Analysis of mercury.**

18 The water-soluble Hg (representing Hg bioavailability) in paddy soils was extracted according to Shi et
19 al. with slight modifications (Shi et al., 2005). Briefly, ~0.5 g of soil was extracted in 8 mL of Milli-Q
20 water with continuous agitation for 2 h. The suspension was centrifuged at 2850 g for 30 min and vacuum
21 filtered through 0.45- μm mixed cellulose acetate filters (Whatman, USA). The amount of water-soluble
22 Hg in solution was measured by cold vapor atomic fluorescence spectrometry (CVAFS, Brooks Rand
23 Model III, Brooks Rand Laboratories) according to USEPA method 1631 (EPA, 2002). To determine
24 total Hg (THg), ~0.2 g of soil was digested in 5 mL of freshly prepared aqua regia ($\text{HCl}:\text{HNO}_3 = 3:1$ v/v)
25 with 5 mL of Milli-Q water at 95 °C for 55 mins. The total Hg amount in the digest solution was
26 measured by cold vapor atomic fluorescence spectrometry (CVAFS, Brooks Rand Model III, Brooks
27 Rand Laboratories) according to USEPA method 1631 (EPA, 2002). Approximately 0.3-0.4 g of soil was

28 extracted using CuSO_4 -methanol solvent for MeHg quantification via gas chromatography CVAFS
29 (GC-CVAFS, Brooks Rand Model III, Brooks Rand Laboratories) following the procedure of USEPA
30 method 1630 (EPA, 2001). To ensure the accuracy of THg and MeHg quantification in soils, method
31 blanks and standard reference materials, GSS-5 (THg: $290 \pm 30 \text{ ng g}^{-1}$) and ERMCC580 (MeHg: $75.5 \pm$
32 3.7 ng g^{-1}), were analyzed. The THg and MeHg recoveries from GSS-5 and ERMCC580 were $113.0\% \pm$
33 7.1% ($n=6$) and $103.6\% \pm 3.5\%$ ($n = 3$), respectively. The relative standard deviation (RSD%) for THg
34 and MeHg analysis in triplicate was less than 5.2% and 3.9%, respectively.

35 **S1.3 Analysis of dissolved organic matter concentration and composition.**

36 The concentration of soil dissolved organic matter (DOM), reflected by water-soluble dissolved organic
37 carbon, was determined by extracting 1 g of soil with Milli-Q water in a 1:10 w/v ratio. The extract was
38 then filtered using $0.45 \mu\text{m}$ polypropylene membrane filters and analyzed using a total organic carbon
39 analyzer (Vario TOC cube, Elementar, Germany). The dissolved organic matter composition (reflected
40 by optical properties of DOM) was characterized with UV-Vis absorption through Aqualog®
41 absorption-fluorescence spectroscopy (Jobin Yvon, Horiba, Japan) on the same extract used for
42 measuring DOC concentration. UV-Vis absorption spectra for liquid samples were scanned from 230 nm
43 to 800 nm (1 nm interval) (Liu et al., 2022). Internal filtering effects were minimized via
44 pre-measurement dilution to a DOC < 10 mg/L (Jiang et al., 2018). S_R (spectral slope ratio over the
45 ranges of 275-295 nm and 350-400 nm) of DOM was calculated for the optical property of DOM, and the
46 detailed calculation and description can be found in previous works (Jiang et al., 2018; Zhang et al.,
47 2023).

48 **S1.4 Analysis of low-molecular-weight organic acids.**

49 Soils from NMS, MMS and HMS were selected for analysis of low-molecular-weight organic acids. Soil
50 (~10 g) was extracted with 20 mL milli-Q water for 12 h. The mixture was centrifuged at $15\,000 \times g$ for
51 15 min, and filtered through Whatman No. 42. Water-soluble low-molecular-weight organic acids were
52 obtained by evaporating the solvent to dryness in a rotary evaporator at $40 \text{ }^\circ\text{C}$ and redissolving the residue
53 in 1 mL of Mill-Q water. The water-soluble low-molecular-weight organic acids were identified and
54 quantified by using reversed-phase high-performance liquid chromatography (HPLC, Shimadzu LC-20,
55 Shimadzu, Osaka, Japan) with a diode array detector (van Hees et al., 1999).

56 **S2. *hgcA* gene quantification.**

57 The abundance of the *hgcA* gene was quantified with primer set ORNL-Delta-HgcA-F:
58 GCCAACTACAAGMTGASCTWC and ORNL-Delta-HgcA-R: CCSGCNGCRCACCAGACRTT in
59 AB 7500 (Applied Biosystems, USA). The PCR setup was as follows: 10 µl of SYBR Premix Ex Taq
60 (TaKaRa Bio Inc., Japan), 0.5 µL (10 mM) of each primer, 2 µL of diluted DNA template (~20 ng), and 7
61 µL of sterilized DDW (double distilled water). The *hgcA* gene was quantified in triplicate under the
62 following thermal cycles: 3 min initial denaturation at 95°C, 40 cycles of 15 s at 95°C, 15 s at 50°C, and
63 15 s at 55°C, and 4 min at 72°C, followed by a plate read at 83 °C (Liu et al., 2018). Three no-template
64 controls were used to detect contamination during the amplification process.

65 **S3. Bacterial culture and validation experiment.**

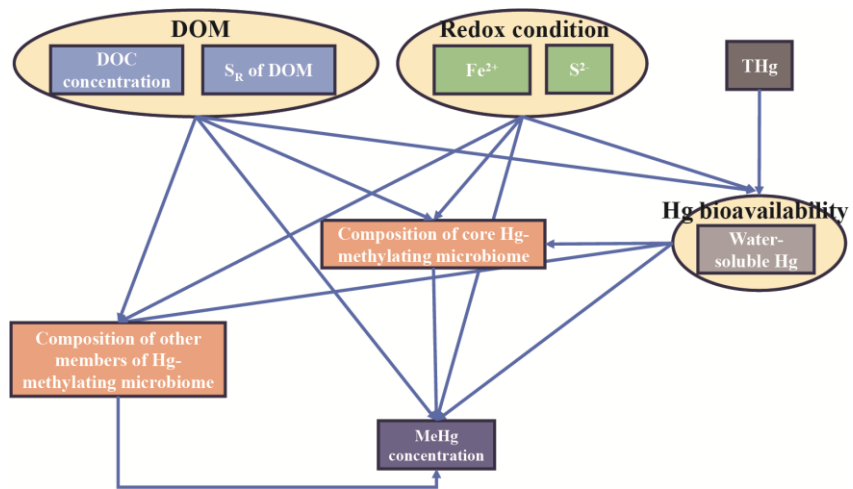
66 *Geobacter sulfurreducens* PCA was cultured in nutrient broth (NB) at 33°C (Hu et al., 2013). Cells were
67 harvested at the middle log phase and washed three times with phosphate buffered saline (PBS,
68 containing 0.137 M sodium chloride, 0.0027 M potassium chloride, 0.01 M sodium phosphate dibasic,
69 and 0.0018 M potassium phosphate monobasic, pH 7.4) media before the validation experiment.

70 The natural DOM solution was extracted from paddy soils from the second sampling campaign.
71 First, we divided the 19 paddy soil samples into NMS, MMS, and HMS based on mercury concentrations
72 (see [Table S1](#) for the classification results). Then, we mixed all paddy soil samples within each group
73 (NMS, MMS, and HMS) in equal proportions to obtain homogenized samples for each group. Next, we
74 extracted the dissolved organic matter from the soil using a soil-to-water ratio of 1:10 (w/v). The
75 extracted solution was then split into two portions: one for the determination of organic matter
76 composition and the other for validation experiments.

77 Serum bottles (100 mL, borosilicate glass bottle; BKMAM Biotechnology, China) were used for the
78 validation experiment in an oxygen-free glovebox (PLASLABS, USA). The experiment was conducted
79 in PBS medium, supplemented with 5 mL of natural DOM solution extracted from paddy soils (i.e., NMS,
80 MMS and HMS), HgCl₂ (1.36 µg/L; Sinopharm Chemical Reagent Co., Ltd., China), and a cell density
81 of 2×10⁸ cells mL⁻¹. All vials were immediately sealed with caps and kept in the dark on shaker. After
82 incubation for 24 h at 33°C, triplicate sample vials were remove from the shaker and preserved at 4°C.
83 An aliquot (10 mL) was filtered through 0.45 µm polyethersulfone (PES) membranes and analyzed for
84 DOM concentration via total organic carbon analyzer (Vario TOC cube, Elementar, Germany). Another
85 aliquot of the sample (3 mL) was acidified with trace metal grade HCl (0.2% (v/v)) and acetic acid (0.5%
86 (v/v)), and analyzed for MeHg. The remaining aliquot was oxidized overnight in BrCl (1% (v/v)) and
87 analyzed for total Hg. Total Hg and MeHg were measured by CVAFS (Brooks Rand Model III, Brooks
88 Rand Laboratories) and cold vapor atomic fluorescence spectrometry (CVAFS, Brooks Rand Model III,
89 Brooks Rand Laboratories), respectively (EPA, 2001; 2002).

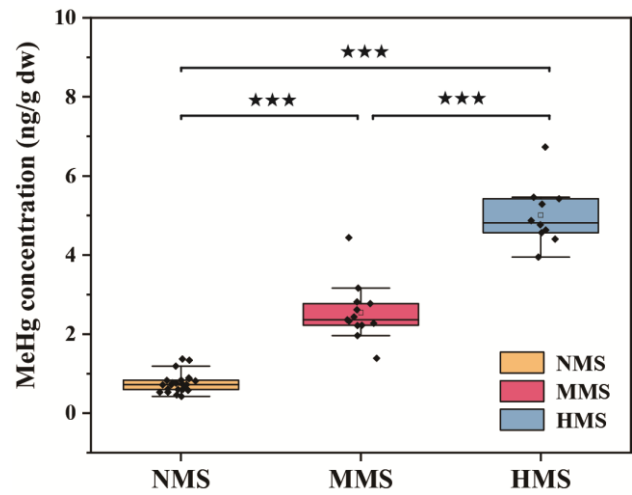
90 To monitor abiotic Hg methylation, the aforementioned experiment was conducted as described
91 above, without addition of bacterial cells.

92 **Supplementary Figures**



93

94 **S1.** *A priori* models for the structure equation models of variation in MeHg production based on the
95 hypothesized causal relationships between multiple factors and MeHg production.

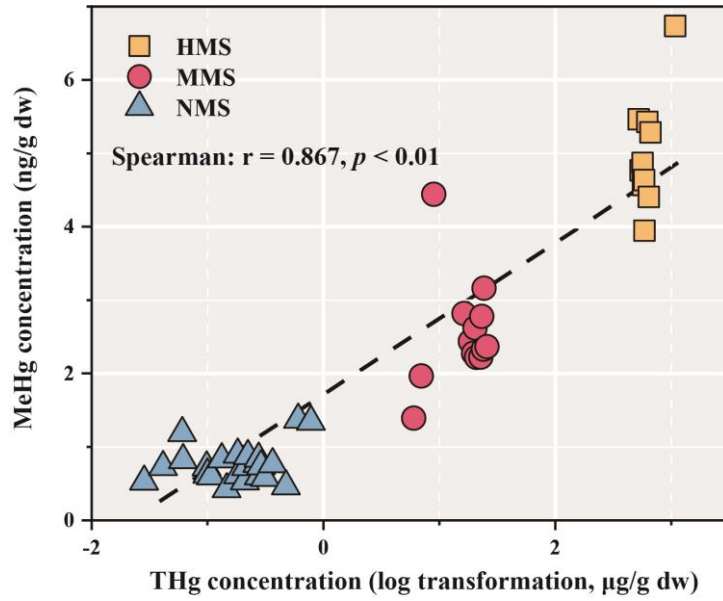


96

97 **S2.** Soil MeHg concentration in paddy soils. NMS, non-Hg polluted paddy soils (n = 23); MMS,

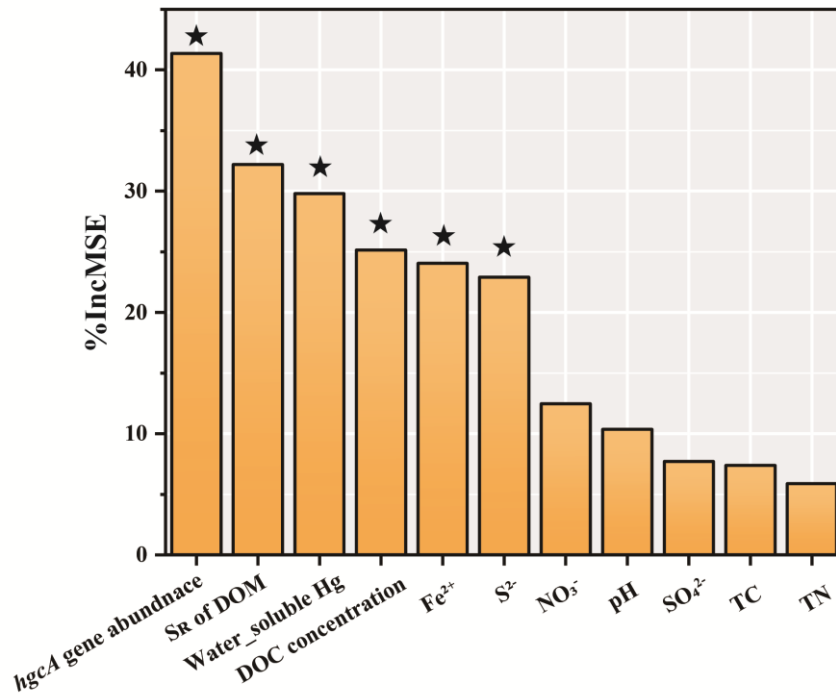
98 moderate Hg-polluted paddy soils (n = 13); HMS, high Hg-polluted paddy soils (n = 10). "****"

99 represents significant difference between different paddy soils ($p < 0.001$).



100

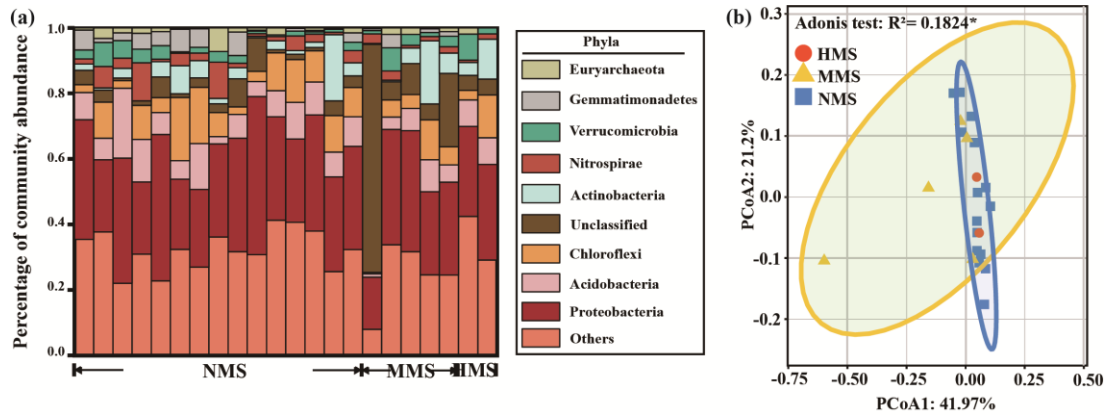
101 **S3.** Correlation between THg and MeHg concentration in paddy soils. NMS, non-Hg polluted paddy
 102 soils (n = 23); MMS, moderate Hg-polluted paddy soils (n = 13); HMS, high Hg-polluted paddy soils (n
 103 = 10).



104

105 **S4.** Random forest modeling indicating the importance of different predictors for MeHg production. The
 106 number of trees used in model is 5000. "★" represents a statistically significant predictor ($p < 0.05$).

107



108

109

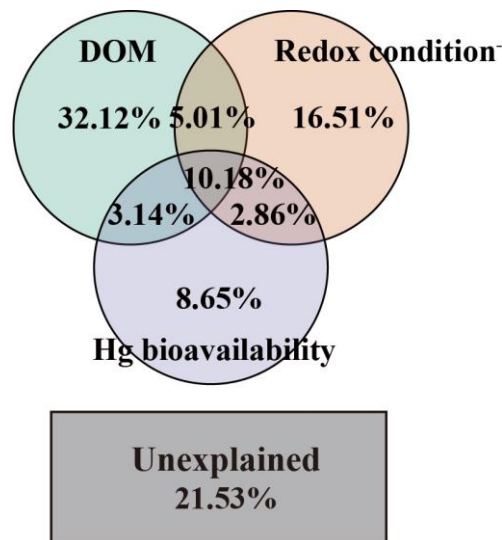
110 **S5.** (a) Hg-methylating microbial community composition in different paddy soils based on

111 metagenomic sequencing. Phyla with low abundance phyla grouped together under "other phyla". (b)

112 Principal coordinates analysis (PCoA) based on Bray-curtis distance showing the overall pattern of

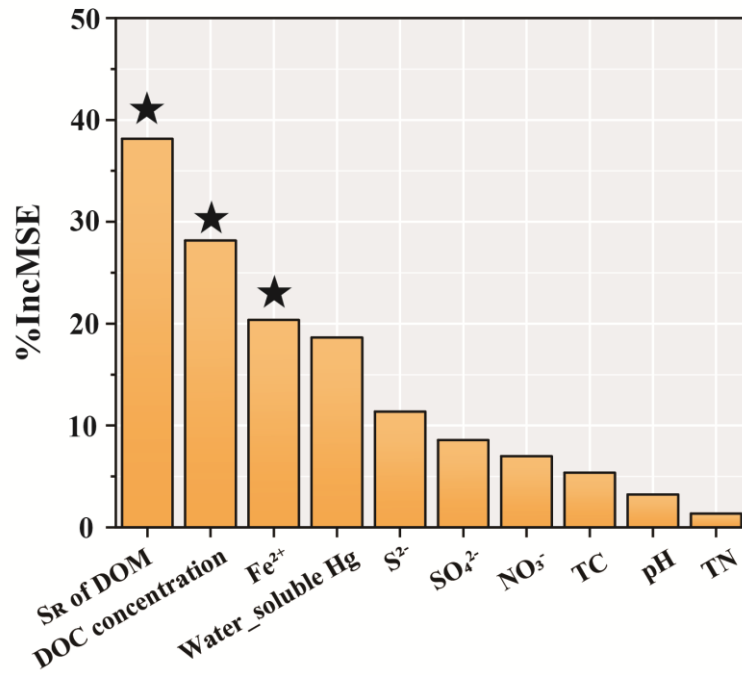
113 Hg-methylating microbial communities in paddy soils. NMS, non-Hg polluted paddy soils (n = 15);

MMS, moderate Hg-polluted paddy soils (n = 5); HMS, high Hg-polluted paddy soils (n = 2).



114

115 **S6.** Variation partitioning analysis differentiating effects of DOM, redox conditions, and Hg
 116 bioavailability on core Hg-methylating microbiome composition. DOM is reflected by DOM
 117 concentration and composition, which are measured as water-soluble DOC concentration and S_R
 118 (spectral slope ratio of $S_{275-295}:S_{350-400}$) values of DOM. Redox conditions are reflected by soil Fe^{2+} and
 119 S^{2-} , which are measured as concentrations of Fe^{2+} and S^{2-} in soil pore water. Hg bioavailability is
 120 reflected by water-soluble Hg. It should be noted that Fe^{2+} and S^{2-} data were limited to the soil samples
 121 obtained in August 2022.



122

123 **S7.** Random forest modeling indicating the importance of different predictors for core Hg-methylating
 124 microbiome composition. The number of trees used in model is 5000. "★" represents a statistically
 125 significant predictor ($p < 0.05$).

127 **S1.** Detailed information for paddy soils collected from 12 provinces across China.

Sample	Province	Site	Longitude	Latitude	Total Hg ($\mu\text{g/g}$)	Sampling time	Category
S1	Guizhou	HX-1	106°31'34"	26°25'15"	0.22	Sep. 2020	NMS
S2	Guizhou	HX-2	106°31'20"	26°25'18"	0.27	Sep. 2020	NMS
S3	Guizhou	HX-3	106°31'21"	26°25'15"	0.29	Sep. 2020	NMS
S4	Guizhou	HX-4	106°31'28"	26°25'16"	0.31	Sep. 2020	NMS
S5	Guizhou	HX-5	106°31'19"	26°25'17"	0.28	Sep. 2020	NMS
S6	Guizhou	HX-6	106°31'26"	26°25'21"	0.28	Sep. 2020	NMS
S7	Guizhou	HX-7	106°31'31"	26°25'20"	0.36	Sep. 2020	NMS
S8	Guizhou	HX-8	106°31'28"	26°25'14"	0.18	Sep. 2020	NMS
S9	Guizhou	HX-9	106°31'15"	26°25'19"	0.21	Sep. 2020	NMS
S10	Guizhou	GX-1	109°09'25"	27°33'23"	19.74	Sep. 2020	MMS
S11	Guizhou	GX-2	109°11'22"	27°33'37"	24.3	Sep. 2020	MMS
S12	Guizhou	GX-3	109°10'09"	27°33'36"	20.24	Sep. 2020	MMS
S13	Guizhou	GX-4	109°12'42"	27°33'53"	23.94	Sep. 2020	MMS
S14	Guizhou	GX-5	109°11'02"	27°33'28"	22.79	Sep. 2020	MMS
S15	Guizhou	GX-6	109°13'38"	27°33'56"	25.67	Sep. 2020	MMS
S16	Guizhou	GX-7	109°10'35"	27°33'33"	23.25	Sep. 2020	MMS
S17	Guizhou	GX-8	109°09'55"	27°33'43"	20.86	Sep. 2020	MMS
S18	Guizhou	GX-9	109°09'12"	27°33'31"	18.56	Sep. 2020	MMS
S19	Guizhou	SK-1	109°12'34"	27°30'41"	639.87	Sep. 2020	HMS
S20	Guizhou	SK-2	109°12'48"	27°31'05"	586.56	Sep. 2020	HMS
S21	Guizhou	SK-3	109°12'24"	27°30'36"	524.16	Sep. 2020	HMS
S22	Guizhou	SK-4	109°12'27"	27°30'25"	543.04	Sep. 2020	HMS
S23	Guizhou	SK-5	109°12'35"	27°30'39"	583.72	Sep. 2020	HMS
S24	Guizhou	SK-6	109°12'18"	27°30'50"	567.14	Sep. 2020	HMS
S25	Guizhou	SK-7	109°12'30"	27°30'52"	621.2	Sep. 2020	HMS
S26	Guizhou	SK-8	109°12'38"	27°30'55"	570.8	Sep. 2020	HMS
S27	Guizhou	SK-9	109°12'49"	27°31'02"	661.62	Sep. 2020	HMS
S28	Jilin	5N-3	125°57'0"	43°42'54"	0.03	Aut. 2022	NMS
S29	Jilin	5N-8	125°44'7"	44°6'26"	0.06	Aut. 2022	NMS
S30	Liaoning	5M-5	123°6'45"	41°49'46"	0.04	Aut. 2022	NMS
S31	Hubei	3I-1	113°10'48"	29°31'48"	0.06	Aut. 2022	NMS
S32	Guangxi	1A-28	108°45'58"	21°48'23"	0.1	Aut. 2022	NMS
S33	Hunan	3I-11	112°24'0"	28°34'12"	0.1	Aut. 2022	NMS
S34	Guangdong	1B-14	110°43'25"	21°51'23"	0.11	Aut. 2022	NMS
S35	Guangxi	1A-22	110°14'59"	22°21'20"	0.13	Aut. 2022	NMS
S36	Sichuan	3K-3	104°20'24"	30°49'12"	0.15	Aut. 2022	NMS
S37	Guizhou	4G-15	106°20'28"	26°25'59"	0.18	Aut. 2022	NMS
S38	Jiangsu	2E-11	119°9'29"	33°28'45"	0.21	Aut. 2022	NMS
S39	Hunan	3I-18	109°38'24"	28°37'12"	0.48	Aut. 2022	NMS
S40	Guangxi	1A-1	109°45'33"	23°11'26"	0.61	Aut. 2022	NMS
S41	Zhejiang	2D-5	119°41'31"	30°19'6"	0.78	Aut. 2022	NMS
S42	Liaoning	5M-1	123°7'9"	41°19'15"	6.01	Aut. 2022	MMS
S43	Shaannxi	6Q-23	109°27'55"	33°5'1"	7	Aut. 2022	MMS
S44	Guizhou	4G-8	109°24'38"	27°39'59"	8.95	Aut. 2022	MMS
S45	Guizhou	4G-7	109°15'13"	27°31'58"	16.34	Aut. 2022	MMS
S46	Chongqin	3J-1	108°55'12"	28°37'48"	1079.75	Aut. 2022	HMS

128 Paddy soils were divided into three categories according to mercury concentration: NMS, non-Hg polluted soils;

129 MMS, moderate Hg-polluted soils; HMS, high Hg-polluted soils. Aut., August; Sep., September.

130 S2. Characterization of dissolved organic matter (DOM) in paddy soils.

Sample	Category	Site	DOM		DOM composition ^a			
			concentration (g kg ⁻¹)	SUVA ₂₅₄	S _R	BIX	FI	HIX
S1	NMS	HX-1	0.36	1.21	1.9	0.63	1.48	0.8
S2	NMS	HX-2	0.36	0.65	0.54	0.69	1.57	0.7
S3	NMS	HX-3	0.37	0.85	1	0.66	1.57	0.73
S4	NMS	HX-4	0.43	1.27	1.28	0.6	1.48	0.78
S5	NMS	HX-5	0.38	0.6	1.2	0.7	1.57	0.71
S6	NMS	HX-6	0.38	1.5	0.99	0.61	1.47	0.83
S7	NMS	HX-7	0.43	0.81	1.2	0.64	1.53	0.76
S8	NMS	HX-8	0.36	0.6	0.51	0.7	1.57	0.71
S9	NMS	HX-9	0.34	1.32	1.7	0.66	1.53	0.76
S10	MMS	GX-1	0.36	1.12	0.77	0.51	1.55	0.99
S11	MMS	GX-2	0.36	0.97	0.82	0.52	1.54	0.98
S12	MMS	GX-3	0.36	0.09	0.79	0.5	1.37	0.88
S13	MMS	GX-4	0.39	1.14	0.93	0.52	1.4	0.98
S14	MMS	GX-5	0.38	1.03	0.92	0.5	1.42	1
S15	MMS	GX-6	0.38	1.01	0.97	0.6	1.59	0.93
S16	MMS	GX-7	0.37	0.63	0.84	0.58	1.5	0.85
S17	MMS	GX-8	0.37	1.08	0.82	0.54	1.42	0.87
S18	MMS	GX-9	0.38	1.14	0.89	0.58	1.5	0.77
S19	HMS	SK-1	0.21	1.04	0.42	0.51	1.17	0.75
S20	HMS	SK-2	0.2	1.08	0.39	0.52	1.19	0.72
S21	HMS	SK-3	0.32	1.32	0.57	0.44	1.08	0.77
S22	HMS	SK-4	0.19	1.53	0.39	0.62	1.24	0.56
S23	HMS	SK-5	0.33	1.15	0.6	0.45	1.2	0.78
S24	HMS	SK-6	0.31	1.48	0.35	0.45	1.12	0.7
S25	HMS	SK-7	0.28	1.59	0.56	0.42	1.06	0.77
S26	HMS	SK-8	0.32	1.16	0.35	0.53	1.2	0.74
S27	HMS	SK-9	0.27	1.15	0.49	0.45	1.2	0.78
S28	NMS	5N-3	0.61	0.16	1.2	0.76	1.63	0.95
S29	NMS	5N-8	0.56	0.12	4.1	0.76	1.57	1
S30	NMS	5M-5	0.54	0.33	1.21	0.94	1.69	0.91
S31	NMS	3I-1	0.5	0.31	1.13	0.63	1.63	0.84
S32	NMS	1A-28	0.64	1.11	0.86	0.57	1.47	0.93
S33	NMS	3I-11	0.51	0.23	1.21	0.65	1.64	0.9
S34	NMS	1B-14	0.55	0.18	1.72	0.57	1.77	0.86
S35	NMS	1A-22	0.51	0.22	2.87	0.83	1.66	0.79
S36	NMS	3K-3	0.58	0.74	1.34	0.54	1.5	0.89
S37	NMS	4G-15	0.33	0.38	1.47	0.56	1.56	0.95
S38	NMS	2E-11	0.5	0.68	1.2	0.5	1.46	0.98
S39	NMS	3I-18	0.45	0.29	0.91	0.55	1.64	0.9
S40	NMS	1A-1	0.89	0.17	1.13	0.73	1.75	0.87
S41	NMS	2D-5	0.54	1.53	1.32	0.73	1.97	0.34
S42	MMS	5M-1	0.39	0.32	0.84	0.58	1.44	0.98
S43	MMS	6Q-23	0.42	0.39	1.06	0.54	1.57	0.92
S44	MMS	4G-8	0.4	0.41	0.99	0.68	1.64	0.79
S45	MMS	4G-7	0.61	0.64	0.93	0.76	1.63	0.95
S46	HMS	3J-1	0.53	1.75	0.52	0.55	1.14	0.62

131 Paddy soils were divided into three categories according to mercury concentration: NMS, non-Hg polluted soils;
 132 MMS, moderate Hg-polluted soils; HMS, high Hg-polluted soils.

133 ^aSUVA₂₅₄ (specific UV absorbance at a wavelength of 254 nm) and S_R (spectral slope ratio of S₂₇₅₋₂₉₅ : S₃₅₀₋₄₀₀) are
 134 properties from UV-Vis absorption spectra of DOM.

135 biological index (BIX), humification index (HIX) and fluorescence index (FI) are the fluorescence compounds and
 136 calculated indices from EEM fluorescence spectra of DOC.

Sample	Category	Site	pH	SO ₄ ²⁻ (mg kg ⁻¹)	NO ₃ ⁻ (mg kg ⁻¹)	TN (%)	TC (%)	S ²⁻ (μM)	Fe ²⁺ (μM)
S1	NMS	HX-1	7.52	347.87	17.67	0.4	5.49	No data	No data
S2	NMS	HX-2	7.53	369.9	19.52	0.28	3.15	No data	No data
S3	NMS	HX-3	7.51	354.61	18.38	0.41	5.47	No data	No data
S4	NMS	HX-4	7.5	369.68	20.26	0.41	5.5	No data	No data
S5	NMS	HX-5	7.52	356.8	18.73	0.21	7.82	No data	No data
S6	NMS	HX-6	7.54	351.22	18.24	0.29	3.13	No data	No data
S7	NMS	HX-7	7.51	358.16	18.76	0.21	7.79	No data	No data
S8	NMS	HX-8	7.53	343.73	18.26	0.29	3.15	No data	No data
S9	NMS	HX-9	7.51	348.69	18.21	0.21	7.77	No data	No data
S10	MMS	GX-1	7.52	348.01	17.62	0.42	5.72	No data	No data
S11	MMS	GX-2	7.52	349.67	17.55	0.21	7.99	No data	No data
S12	MMS	GX-3	7.5	337.66	17.57	0.42	5.74	No data	No data
S13	MMS	GX-4	7.5	371.17	17.78	0.28	3.21	No data	No data
S14	MMS	GX-5	7.49	335.06	17.63	0.43	5.71	No data	No data
S15	MMS	GX-6	7.5	381.51	17.79	0.27	3.19	No data	No data
S16	MMS	GX-7	7.5	333.01	17.6	0.47	6.08	No data	No data
S17	MMS	GX-8	7.51	377.65	17.55	0.21	7.88	No data	No data
S18	MMS	GX-9	7.5	339.97	17.5	0.21	7.93	No data	No data
S19	HMS	SK-1	7.51	254.52	15.65	0.48	6.12	No data	No data
S20	HMS	SK-2	7.48	255.55	14.58	0.21	7.84	No data	No data
S21	HMS	SK-3	7.47	266.23	16.1	0.46	6.1	No data	No data
S22	HMS	SK-4	7.45	271.33	15.52	0.32	4.71	No data	No data
S23	HMS	SK-5	7.51	251.63	15.56	0.28	7.92	No data	No data
S24	HMS	SK-6	7.45	256.33	14.92	0.29	3.14	No data	No data
S25	HMS	SK-7	7.48	246.24	16.06	0.46	6.07	No data	No data
S26	HMS	SK-8	7.45	241.53	14.5	0.22	7.89	No data	No data
S27	HMS	SK-9	7.47	219.44	16.4	0.21	3.18	No data	No data
S28	NMS	5N-3	7.36	393.09	15.91	0.25	2.71	0.87	16752.81
S29	NMS	5N-8	7.68	291.38	18.36	0.18	6.73	0.28	20058.81
S30	NMS	5M-5	6.84	421.42	7.98	0.18	6.7	0.38	34030.78
S31	NMS	3I-1	7.11	296.93	17.07	0.24	2.76	0.92	8490.57
S32	NMS	1A-28	6.95	278.44	17.39	0.36	4.94	1.31	19670.1
S33	NMS	3I-11	6.84	293.2	18.57	0.24	2.71	2.21	3476.21
S34	NMS	1B-14	6.88	286.05	17.68	0.18	6.82	1.38	10140.85
S35	NMS	1A-22	7.48	282.71	17.03	0.18	6.87	1.13	3147.96
S36	NMS	3K-3	7.01	206.27	14.03	0.41	5.26	2.06	1869.54
S37	NMS	4G-15	7.06	268.33	16.82	0.18	6.68	0.87	77.94
S38	NMS	2E-11	6.54	290.39	16.03	0.23	2.74	0.72	1567.21
S39	NMS	3I-18	7.01	293.8	18.55	0.37	4.91	0.46	3912.43
S40	NMS	1A-1	7.12	273.16	15.44	0.18	6.78	0.55	44307.05
S41	NMS	2D-5	7.03	185.56	18.12	0.4	5.23	0.48	64217.64
S42	MMS	5M-1	6.88	250.39	17.8	0.36	4.92	0.85	2849.95
S43	MMS	6Q-23	7.05	394.55	8.76	0.25	2.69	0.55	3031.35
S44	MMS	4G-8	7.52	292.47	18.19	0.35	4.7	0.17	7086.89
S45	MMS	4G-7	5.57	289.84	18.25	0.34	4.72	0.85	17456.81
S46	HMS	3J-1	6.18	436.82	18.86	0.35	4.73	0.75	4433.16

- 138 Paddy soils were divided into three categories according to mercury concentration: NMS, non-Hg polluted soils;
139 MMS, moderate Hg-polluted soils; HMS, high Hg-polluted soils. No data indicate that the concentrations of S²⁻ and
140 Fe²⁺ were unavailable in soil samples from September 2020 (S1-S26).

141 **S4. Key characteristics of co-occurrence networks in paddy soils.**

Category	Connected nodes	Edges	Module	Average degree	Network diameter	Modularity index
NMS	199	3062	6	15.31	9	0.554
MMS	193	1655	11	8.275	7	0.583
HMS	189	1714	11	8.57	7	0.591

142 NMS, non-Hg polluted paddy soils (n = 23); MMS, moderate Hg-polluted paddy soils (n = 13); HMS, high

143 Hg-polluted paddy soils (n = 10).

144 **S5. Identification of major module (also known as core microbiome) in different paddy soils.**

ID	Module	The number of connections to other modules	Relative abundance (%)	Correlation with MeHg concentration	Correlation with %MeHg
NMS	module1	146	34	0.418*	0.787***
	module2	13	23.5	0.164	-0.374
	module3	28	19	0.206	-0.31
	module4	3	16.5	0.189	-0.256
	module5	17	6.5	0.116	-0.186
	module6	0	0.5	0.047	-0.05
MMS	module1	66	27.5	0.503*	0.863**
	module2	84	20.5	0.035	-0.165
	module3	8	17.5	-0.103	0.066
	module4	59	9	0.068	0.051
	module5	5	8	0.206	-0.204
	module6	5	5.5	-0.049	0.106
	module7	5	3	-0.085	0.04
	module8	3	2.5	0.039	-0.065
	module9	0	2	0.101	-0.169
	module10	1	1	-0.008	0.016
	module11	0	3.5	0.026	-0.064
HMS	module1	161	20	0.410*	0.872**
	module2	120	18.5	-0.351	0.531
	module3	0	16.5	0.318	-0.518
	module4	25	9.5	-0.113	0.219
	module5	43	9	-0.259	0.654*
	module6	29	7.5	-0.302	0.518
	module7	0	5	-0.101	0.215
	module8	0	3.5	0.002	-0.008
	module9	0	1.5	-0.029	0.126
	module10	0	1.5	-0.106	0.204
	module11	0	7.5	0.284	-0.579

145 NMS, non-Hg polluted paddy soils (n = 23); MMS, moderate Hg-polluted paddy soils (n = 13); HMS, high

146 Hg-polluted paddy soils (n = 10).

147

148

149 **References:**

- 150 Cline, J. D.: Spectrophotometric determination of hydrogen sulfide in natural waters¹, *Limnol.*
151 *Oceanogr.*, 14, 454-458, <https://doi.org/10.4319/lo.1969.14.3.0454>, 1969.
- 152 EPA, U.: Method 1630: Methyl Mercury in Water by Distillation, Aqueous Ethylation, Purge and Trap,
153 and Cold Vapor Atomic Fluorescence Spectrometry CVAFS (EPA-821-R-01-020), United States
154 Environmental Protection Agency, Washington, DC,
155 https://www.epa.gov/sites/default/files/2015-08/documents/method_1630_1998.pdf, 2001.
- 156 EPA, U.: Method 1631, Revision E: Mercury in Water by Oxidation, Purge and Trap, and Cold Vapor
157 Atomic Fluorescence Spectrometry (EPA-821-R-02-019), United States Environmental Protection
158 Agency, Washington, DC,
159 https://www.epa.gov/sites/default/files/2015-08/documents/method_1631e_2002.pdf, 2002.
- 160 Hu, H., Lin, H., Zheng, W., Tomanicek, S. J., Johs, A., Feng, X., Elias, D. A., Liang, L., and Gu, B.:
161 Oxidation and methylation of dissolved elemental mercury by anaerobic bacteria, *Nat. Geosci.*, 6,
162 751-754, <https://doi.org/10.1038/ngeo1894>, 2013.
- 163 Jiang, T., Bravo, A. G., Skyllberg, U., Björn, E., Wang, D. Y., Yan, H., and Green, N. W.: Influence of
164 dissolved organic matter (DOM) characteristics on dissolved mercury (Hg) species composition in
165 sediment porewater of lakes from southwest China, *Water Res.*, 146, 146-158,
166 <https://doi.org/10.1016/j.watres.2018.08.054>, 2018.
- 167 Liu, J., Zhao, L., Kong, K., Abdelhafiz, M. A., Tian, S., Jiang, T., Meng, B. and Feng, X.: Uncovering
168 geochemical fractionation of the newly deposited Hg in paddy soil using a stable isotope tracer, *J.*
169 *Hazard. Mater.*, 433, 128752-128752, <https://doi.org/10.1016/j.jhazmat.2022.128752>, 2022.
- 170 Liu, Y., Johs, A., Li, B., Lu, X., Hu, H., Sun, D. H., He, J. Z., and Gu, B.: Unraveling Microbial
171 Communities Associated with Methylmercury Production in Paddy Soils, *Environ. Sci. Technol.*, 52,
172 13110-13118, <https://doi.org/10.1021/acs.est.8b03052>, 2018.
- 173 Shi, J. B., Liang, L. N., Jiang, G. B. and Jin, X. L.: The speciation and bioavailability of mercury in
174 sediments of Haihe River, China, *Environ. Int.*, 31, 357-365,
175 <https://doi.org/10.1016/j.envint.2004.08.008>, 2005.
- 176 van Hees, P. A. W., Dahlén, J., Lundström, U. S., Borén, H. and Allard, B.: Determination of low
177 molecular weight organic acids in soil solution by HPLC, *Talanta*, 48, 173-179,
178 [https://doi.org/10.1016/S0039-9140\(98\)00236-7](https://doi.org/10.1016/S0039-9140(98)00236-7), 1999.
- 179 Viollier, E., Inglett, P. W., Hunter, K., Roychoudhury, A. N. and Van Cappellen, P.: The ferrozine method
180 revisited: Fe(II)/Fe(III) determination in natural waters, *Appl. Geochem.*, 15, 785-790,
181 [https://doi.org/10.1016/S0883-2927\(99\)00097-9](https://doi.org/10.1016/S0883-2927(99)00097-9), 2000.
- 182 Zhang, S., Yin, Y., Yang, P., Yao, C., Tian, S., Lei, P., Jiang, T. and Wang, D.: Using the end-member
183 mixing model to evaluate biogeochemical reactivities of dissolved organic matter (DOM):
184 autochthonous versus allochthonous origins, *Water Res.*, 232, 119644,
185 <https://doi.org/10.1016/j.watres.2023.119644>, 2023.
- 186